

# An example SEG expanded abstract

Joe Dellinger\*, BP and Sergey Fomel, University of Texas at Austin

## SUMMARY

This is an example of using segabs.cls for writing SEG expanded abstracts.

## INTRODUCTION

This is an introduction. L<sup>A</sup>T<sub>E</sub>X is a powerful document typesetting system (Lamport, 1994). An excellent reference is (Kopka and Daly, 2004). The new segabs.cls class complies with the L<sup>A</sup>T<sub>E</sub>X2e standard.

## DATA AND METHODS

The data mostly come from portable broad-band stations of the Brazilian Lithosphere Seismic Project, deployed across several parts of Brazil since 1992. and publicly available from the IRIS (Incorporated Research Institutions for Seismology) data management system. A few permanent stations of the Global Seismographic Network and the GEOSCOPE network are also included (Fig. 1). Specifically, our data set contains 53 stations from which we select the vertical component, thus focusing the study on Rayleigh waves. The seismic records span a 16-yr interval, from 1996 to 2012. As Fig. 1 shows, the stations most densely cover central and southeastern Brazil, that is, the So Francisco craton, the adjacent Tocantins and Mantiqueira provinces and the Paran basin. This being said, stations located further to the north are crucial to provide coverage of the Amazon craton, the Parnaba basin and the Borborema province.

### Cross-correlation

As mentioned in the Introduction, the cross-correlation function  $AB(\tau)$  between the ambient noise  $u_A(t)$ ,  $u_B(t)$  recorded at two seismic stations located at A and B,

Here are examples of equations involving vectors and tensors:

$$\mathbf{R} = \begin{pmatrix} R_{XX} & R_{YX} \\ R_{XY} & R_{YY} \end{pmatrix} = \mathbf{P}_{M \rightarrow R} \mathbf{D} \mathbf{P}_{S \rightarrow M} \mathbf{S} \quad , \quad (1)$$

and

$$R_{j,m}(\omega) = \sum_{n=1}^N P_j^{(n)}(\mathbf{x}_R) D^{(n)}(\omega) P_m^{(n)}(\mathbf{x}_S) \quad . \quad (2)$$

tends to the Greens function between A and B (Shapiro & Campillo 2004): the positive lag part of  $AB(\tau)$  gives the response at B to an impulse located at A, and vice versa for the negative lag part. In practice, several signal processing steps are required before the cross-correlation between each pair of stations can be estimated. We follow in the present work the steps advocated by Bensen et al. (2007), which consist in stacking daily cross-correlations after (1) removing the

instrument response, the mean and the trend, (2) band-pass filtering the data between 760 or 360 s, (3) downsampling the signal to 1 Hz, (4) normalizing the signal by the running average of its absolute values and (5) whitening the Fourier amplitude spectrum in the considered frequency band.

In step 2, we found that periods up to at least 60 s must be retained in the waveforms in order to maximize the signal-to-noise ratios (SNRs) of the cross-correlations up to periods 2025 s. Furthermore, the period band 360 s serves to produce the group velocity map at the shortest periods, 6 and 10 s (see Section 2.4), but we observed that the inclusion of high frequencies yields spectral leakage effects that significantly degrade the SNRs at periods larger than 10 s. The tomographic inversions at longer periods are therefore based on the data bandpass filtered between 7 and 60 s. Further work is needed to identify the causes of the spectral leakage, which we suspect to be related to the time-domain normalization (step 4). This step is intended to minimize the influence of phenomena that obscure ambient noise, such as earthquakes and instrumental irregularities. Bensen et al. (2007) note that the normalization weights may be computed from the waveform bandpass filtered in the earthquake period band in order to better remove earthquakes close to the noise level. As the level of seismicity is not significant in the studied region, this did not yield any improvement on our data (and even slightly degraded the SNRs at short periods), and we thus normalized the signal using the entire considered period band. Many studies apply the one-bit normalization technique, wherein only the sign of the signal is retained (+1 or -1) and the amplitude is disregarded completely (e.g. Shapiro & Campillo 2004; Picozzi et al. 2009; Huang et al. 2010). We found that the running-absolute-mean normalization yields much higher SNRs than the one-bit normalization on our data set, which is in agreement with the results of Seats et al. (2012).

Fig. 2 shows all the available cross-correlations, normalized to unity and stacked as a function of the inter-station distance. Arrival times corresponding to propagation speeds between 2.5 and 3.5 km/s clearly emerge from the cross-correlations. As a last step before measuring the dispersion curves, the cross-correlations are symmetrized and turned into one-sided signals by averaging the positive and the negative lag parts. This symmetrization method was applied in most previous studies, but alternative techniques could be tested in future research: for example, discarding of the side with the lowest SNR (Pawlak et al. 2011) or phase coherence weighting (Schimmel & Gallart 2007; Dias et al. 2015).

## Figures

Figure 1 shows what it is about.

### Multiplot

Sometimes it is convenient to put two or more figures from

## SEG abstract example

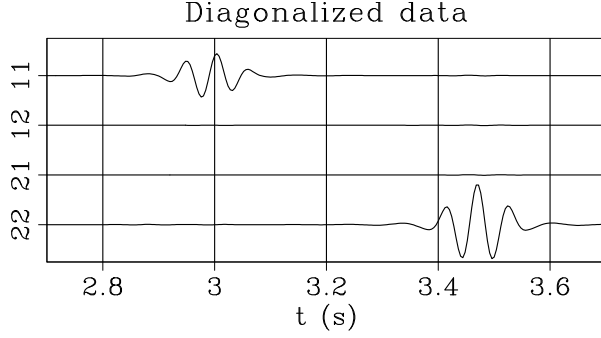


Figure 1: This figure is specified in the document by `\plot{waves}{width=\columnwidth}{This caption.}`.

different files in an array (see Figure 2). Individual plots are Figures 2a and 2b.

The first argument of the `multiplot` command specifies the number of plots per row.

### Tables

The discussion is summarized in Table 1.

Table Example		
migration	$\omega \rightarrow k_z$	$k_y^2 + k - z^2 \cos^2 \psi = 4\omega^2/v^2$
zero-offset diffraction	$k_z \rightarrow \omega_0$	$k_y^2 + k_z^2 = 4\omega_0^2/v^2$
DMO+NMO	$\omega \rightarrow \omega_0$	$\frac{1}{4}v^2k_y^2 \sin^2 \psi + \omega_0^2 \cos^2 \psi = \omega^2$
radial DMO	$\omega \rightarrow \omega_s$	$\frac{1}{4}v^2k_y^2 \sin^2 \psi + \omega_s^2 = \omega^2$
radial NMO	$\omega_s \rightarrow \omega_0$	$\omega_0 \cos \psi = \omega_s$

Table 1: This table is specified in the document by `\tabl{example}{This caption.}{...}`.

### ACKNOWLEDGMENTS

I wish to thank Ivan Pšenčík and Frédéric Billette for having names with non-English letters in them. I wish to thank Červený (2000) for providing an example of how to make a bib file that includes an author whose name begins with a non-English character and Forgues (1996) for providing both an example of referencing a Ph.D. thesis and yet more non-English characters.

### APPENDIX A

#### APPENDIX EXAMPLE

According to the new SEG standard, appendices come before references.

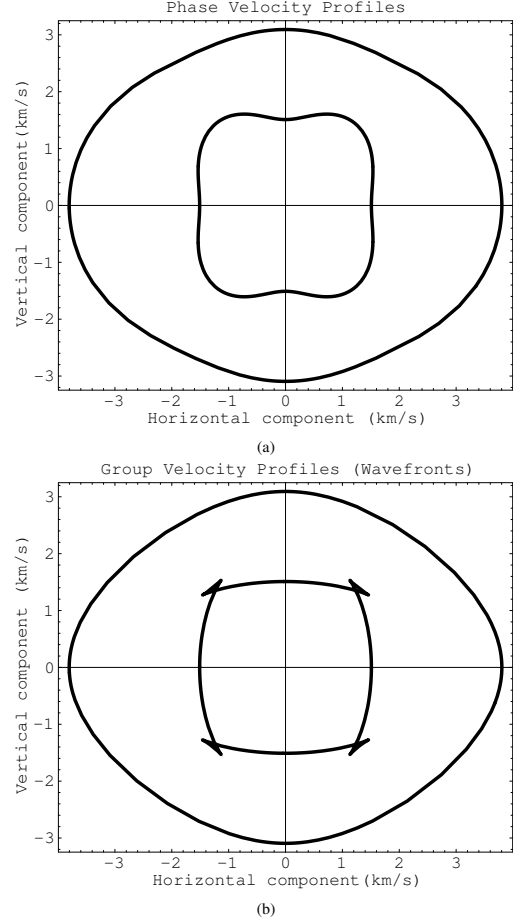


Figure 2: This figure is specified in the document by `\multiplot{2}{exph,exgr}{width=0.4\textwidth}{This caption.}`.

## SEG abstract example

$$\frac{\partial U}{\partial z} = \left\{ \sqrt{\frac{1}{v^2} - \left[ \frac{\partial t}{\partial g} \right]^2} + \sqrt{\frac{1}{v^2} - \left[ \frac{\partial t}{\partial s} \right]^2} \right\} \frac{\partial U}{\partial t} \quad (\text{A-1})$$

It is important to get equation A-1 right.

## APPENDIX B

### ANOTHER APPENDIX

$$\frac{\partial U}{\partial z} = \left\{ \sqrt{\frac{1}{v^2} - \left[ \frac{\partial t}{\partial g} \right]^2} + \sqrt{\frac{1}{v^2} - \left[ \frac{\partial t}{\partial s} \right]^2} \right\} \frac{\partial U}{\partial t} \quad (\text{B-1})$$

Too lazy to type a different equation but note the numeration.

The error comparison is provided in Figure B-1.

# SEG abstract example

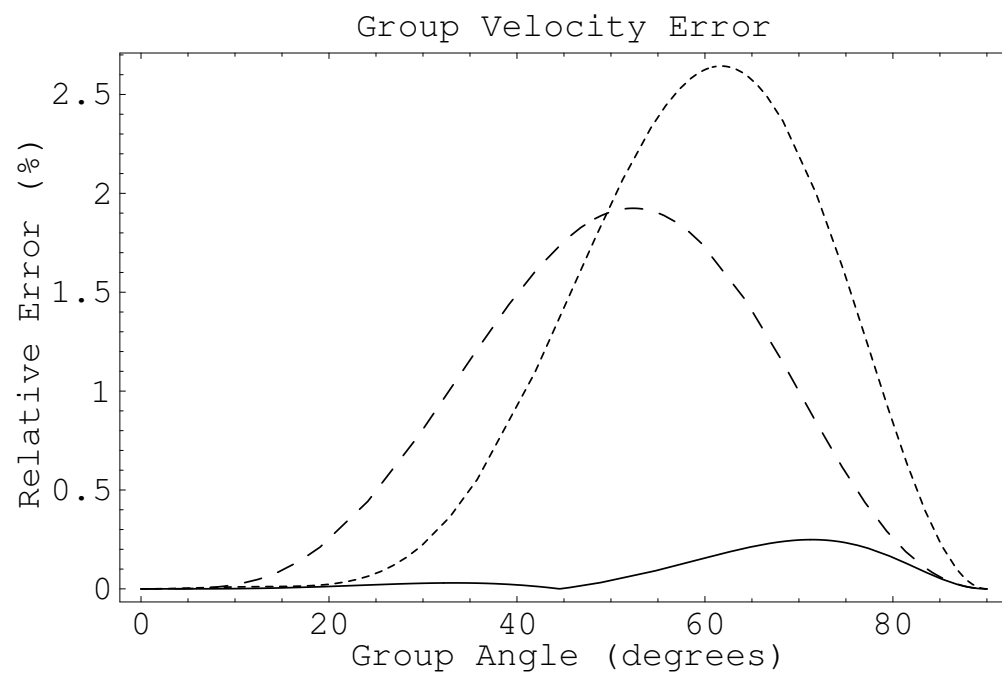


Figure B-1: This figure is specified in the document by `\plot*{errgrp}{width=0.8\textwidth}{This caption.}`.